Computation

CrossMark

Surrogate models of the influence of the microstructure on the mechanical properties of closed- and open-cell foams

M. Marvi-Mashhadi[1,2], C. S. Lopes[1], and J. LLorca[1,2,*]

[1] *IMDEA Materials Institute, C/ Eric Kandel 2, 28906 Getafe, Madrid, Spain*

[2] *Department of Materials Science, Polytechnic University of Madrid/Universidad Politécnica de Madrid, E. T. S. de Ingenieros de Caminos, 28040 Madrid, Spain*

ABSTRACT

The mechanical behavior of closed- and open-cell foams was analyzed using a computational homogenization strategy based on the finite element simulation of a representative volume element of the foam microstructure. The representation of the foam took into account the main microstructural features, namely density, fraction of solid material in cell walls and struts, cell anisotropy, cell size and distribution and strut shape. A parametric study was carried out to ascertain the influence of these parameters on the elastic modulus and the plateau stress under compression. It was found that these properties mainly depended on the density, fraction of solid material in cell walls and struts and cell anisotropy. Building upon the results of the parametric study, surrogate models were developed to relate the influence of the microstructure on the mechanical properties of the foams. It is believed that these models can be used for the design of foams with optimized properties for particular applications.

Introduction

Polymeric and metallic foams are used in many structural applications in engineering due to their low density, large elastic deformability as well as energy absorption under impact [1–5]. One important feature of foams is that their properties can be tailored by changing the physical parameters that determine the foam microstructure, such as density, cell size and aspect ratio, fraction of open and close

cells in addition to the properties of the solid material in the foam.

In the particular case of the mechanical properties, the relationship between microstructure and mechanical properties has been analyzed in detail by means of the computational homogenization of a representative volume element (RVE) of the foam microstructure [6]. The ability of this strategy to reproduce accurately the mechanical properties of foams has increased dramatically over the years as more realistic RVEs were used for the simulations. In

Address correspondence to E-mail: javier.llorca@imdea.org

Springer

particular, the topology of the foam microstructure (average number of faces per cell and the average number of edges per face) and the variability in the cell size distribution were captured by spatial representations of the foam microstructure based on 3D Voronoi or Laguerre tessellations [6–11], while other important details (strut shape, cell anisotropy, mass distribution between cell walls and struts, etc.) could also be taken into account. The capability of these models to establish the influence of the microstructure of foams on mechanical properties has been demonstrated recently. In particular, the cell size distribution and strut shape were obtained by means of X-ray microtomography, while the cell wall thickness was determined by means of scanning electron microscopy and the mechanical properties of the solid polyurethane in the foam were determined by means of instrumented nanoindentation [11]. This information was used to build realistic RVEs of the foam microstructure, which provided accurate predictions of the elastic modulus [7] and, more recently, of the plateau stress under compression [11], including the effect of anisotropy [12].

It should be noted, however, that computational homogenization of realistic RVEs is expensive and cannot be used to perform fast and accurate assessments of the effect of microstructure on the mechanical properties of the foams that can be used during either component design or material optimization processes. These tasks require surrogate models based on simple analytical expressions that relate the most relevant microstructural factors with the mechanical properties. The pioneer work in this direction was developed by [13] based on the analysis of a simple cubic cell structure. They provided the following expressions for elastic modulus, E, and the yield strength in compression, σ_y, of close cell foams with the density of ρ as

$$\frac{E}{E_s} = C_1 \phi^2 \left(\frac{\rho}{\rho_s}\right)^2 + C_1'(1-\phi)\frac{\rho}{\rho_s} \tag{1}$$

$$\frac{\sigma_y}{\sigma_{ys}} = C_3 \left(\phi \frac{\rho}{\rho_s}\right)^{1.5} + C_4(1-\phi)\frac{\rho}{\rho_s} \tag{2}$$

where E_s, σ_{ys} and ρ_s are the stiffness, yield strength and density of the solid material, respectively, and ϕ is the volume fraction of solid material in the struts. C_1, C_1', C_3 and C_4 are coefficients which were calibrated to fit the experimental values. It should be noted, however, that the predictions of these models could only provide general trends because of the

simplicity of the geometrical model and the underlying assumptions, and were not accurate in many cases [10, 13].

More recently, Köll and Hallström [10] carried out a parametric study based on computational homogenization to determine the stiffness of closed-cell foams as a function of ρ and ϕ. The RVEs were built from an initial Voronoi tessellation of the space, and the generated Voronoi partitions were transformed into dry foams with a minimum total surface area. The mass of the solid material was distributed between the cell faces and the struts, which have a constant three-cuspid cross sections. The results of the parametric study were used to modify Eq. (1) to get a better agreement with the predictions of the numerical simulations according to

$$\frac{E}{E_s} = f(\phi)\left(\frac{\rho}{\rho_s}\right)^2 + g(\phi)\frac{\rho}{\rho_s} \tag{3}$$

where

$$f(\phi) = a\phi^2 + b\phi + c$$
$$g(\phi) = d\phi + e \tag{4}$$

and the values of parameters a, b, c, d and e can be found in [10]. The simulations also indicated that the variation of the cell size distribution did not influence the stiffness of the foam.

In the present work, the modeling strategy based on computational homogenization, developed previously in [11, 12], is used to carry out a parametric study of the influence of foam density, distribution of the solid material between walls and struts, cell size distribution, strut shape as well as cell anisotropy on the stiffness and yield strength in compression (plateau stress) of close cell foams. The results of the parametric study were used to develop new surrogate models, in the spirit of Eqs. (1) and (2), to relate the microstructural features of the foam to the macroscopic properties.

The paper is structured as follows. The simulation methodology is briefly recalled in Sect. 2 for the sake of completion and to define the microstructural parameters in the model. The results of the parametric study are presented in Sect. 3, while the new surrogate models for the elastic modulus and yield strength are presented and proposed according to the results of the parametric study in Sect. 4. The conclusions and future work are finally summarized in Sect. 5.

Computational homogenization strategy

Marvi-Mashhadi et al. [11, 12] developed a methodology to determine the mechanical properties of foams based on computational homogenization of an RVE of the foam microstructure (Fig. 1). Starting from the experimental data of cell size distribution (which followed a Gaussian distribution), the topology of the foam was built by means of a Laguerre tessellation in a cubic domain [11]. The Laguerre tessellation is a weighted generalization of the standard Voronoi tessellation in which the space is divided into convex, space-filling polyhedrons which intersect only in their boundaries. The input information for the Laguerre tessellation is the position and the weights of the seed points for the tessellation. They can be obtained from position of the centers and the radii, respectively, of an ensemble of random closed-packed polydisperse spheres whose size distribution follows that of the cell size distribution in the foam [14, 15]. The cell size distribution obtained with this technique was isotropic (Fig. 1a), and
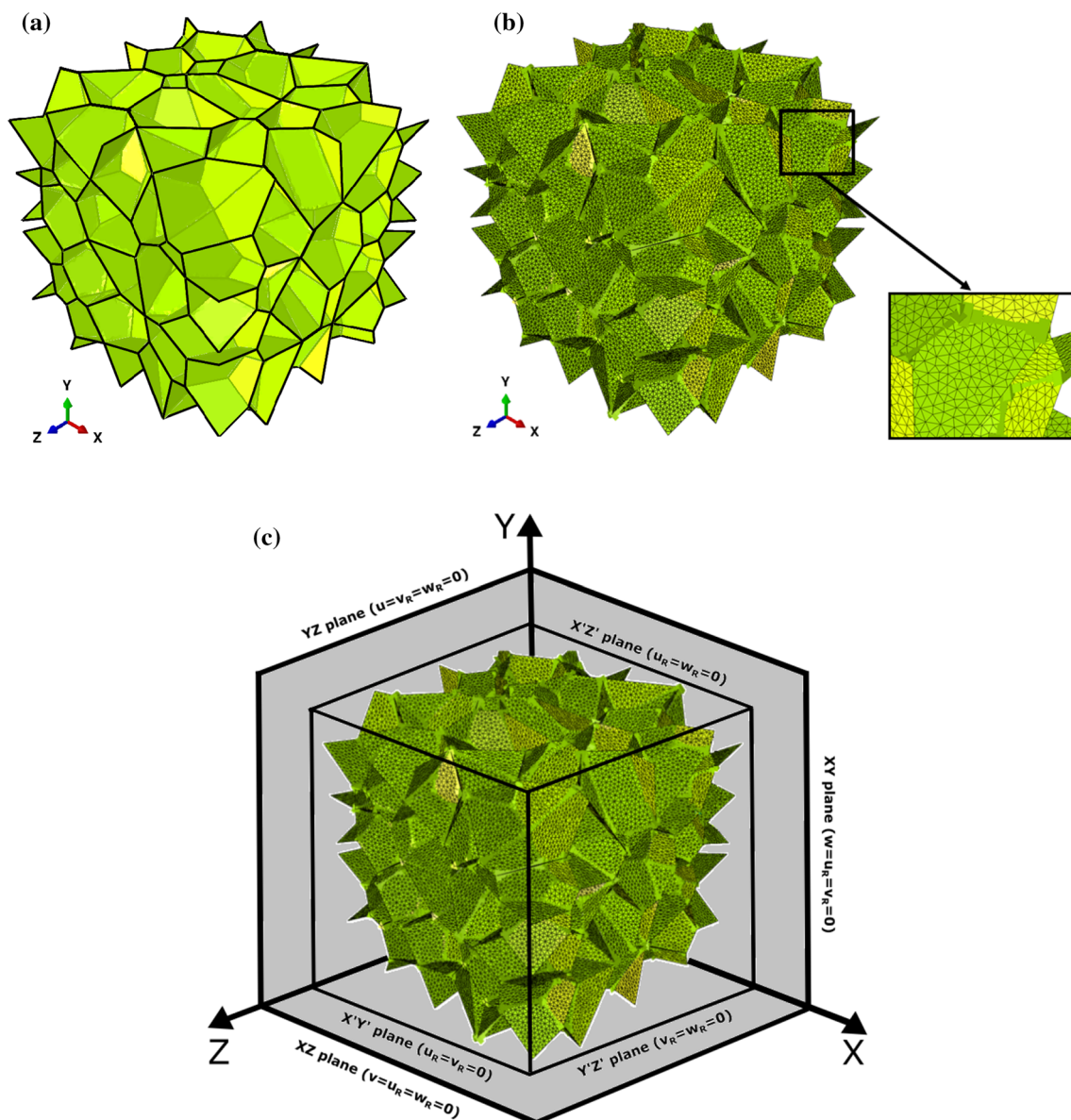

Figure 1 Summary of the computational homogenization modeling strategy. **a** Topology of an RVE of the closed-cell foam obtained by means of Laguerre tessellation. **b** Finite element discretization of the RVE using shell element for the cell walls and beam elements for the struts. **c** Schematic of the boundary conditions used in the simulation of the RVE.

structural anisotropy of the foam in one direction was included by means of the affine deformation of all the nodes in the RVE by a factor s. The RVEs included 100 cells because it was shown in [11] that this number of cells was large enough to provide average values of the elastic stiffness and the plateau stress that were independent of the RVE size.

Cell walls and struts of the model were discretized for the numerical simulation with the finite element method (Fig. 1b). Shell elements (type S3R in [16]) were used for the cell walls and beam elements (Euler–Bernoulli type B31 in [16]) for the struts. The shell element thickness was constant throughout the RVE. The beam element section was an equilateral triangle (that can be approximated from the trapezoidal section in Abaqus), which is the closest one to the three-cusp hypocycloid cross section of struts in the foam microstructure [17]. Each strut was discretized with a number of beam elements with different cross-sectional area, so the strut shape followed Eq. (5),

$$A = A_0 f(x/L) = A_0 \left[5.45 \left(\frac{x}{L} \right)^4 + 2.63 \left(\frac{x}{L} \right)^2 + 1.00 \right]$$

(5)

where A stands for a cross-sectional area of the strut at position x along the strut with the length of L and the area at the mid-span of A_0. This expression was obtained as the average from the analysis of the strut shape by means of X-ray computed tomography in a polyurethane foam [11]. Around 22 beam elements were used to discretize a strut of average length in the case of isotropic foams, while 30–40 elements were used for anisotropic foams. These numbers were large enough to obtain results of the mechanical response that were independent of the finite element discretization [11, 12].

The total mass of the solid material in the foam was given by the relative density of the foam, and it was distributed between the struts and the cell walls. The volume of solid material in the cell walls was given by the shell element thickness (equal to the cell wall thickness), while the remaining solid material was attached to the struts assuming that the volume of each strut was proportional to its length.

Numerical simulations of the mechanical behavior of the RVEs in compression were carried out using Abaqus explicit [16] within the framework of the finite deformations and rotations theory with the

initial unstressed state as reference (Fig. 1c). The solid material was modeled as an isotropic, elastic-perfectly plastic solid following the J_2 theory of plasticity, characterized by the elastic constants (E_s and $v = 0.35$) and the yield stress, σ_{ys}. Simulations were performed under quasi-static conditions, and this situation was monitored by checking the kinetic energy (less than 2% of the total energy) and the reaction forces on opposite surfaces. The rotational degrees of freedom (u_R, v_R, w_R) around the axes contained in each of the 6 boundary faces of the model were constrained. In addition, the translational degrees of freedom normal to three of the faces of the RVE were constrained, i.e., planes YZ ($u = 0$), XZ ($v = 0$) and XY ($w = 0$), Fig. 1c. The compression load was applied by means of the relative displacement of rigid surfaces (load-plates) in contact with the RVE at the faces XZ and $X'Z'$. In this way, the elements of the model were prevented from overlapping the boundaries of RVE as a result of buckling. The friction between the rigid surfaces and the RVE was neglected. More details about the modeling strategy can be found in [11].

Parametric study

The mechanical behavior of the foam in compression was determined by means of the finite element analysis of RVEs with 100 cells. The stress–strain curves in compression obtained from three different cell realizations in the RVE are plotted in Fig. 2a) for an isotropic foam to illustrate the results of the modeling strategy. They were obtained for closed-cell foams with nominal relative densities of 2.52% and 2.91%, average cell sizes of 216 ± 67 μm and 490 ± 128 μm, fraction of the mass in the struts of 79% and 85% for isotropic and anisotropic foams, respectively. The initial elastic deformation was followed by a nonlinear regime up to a maximum in the stress which marked the onset of plastic instability triggered by the plastic buckling of the struts in one section of the foam [12]. The elastic modulus and the plateau stress (define as the stress at the onset of plastic instability) could be obtained from these curves, and the simulations were finished after the onset of plastic instability was attained.

The mechanical response of an anisotropic foam ($s = 1.57$) in two directions (parallel and perpendicular to the longest cell axis) is plotted in Fig. 2b). The
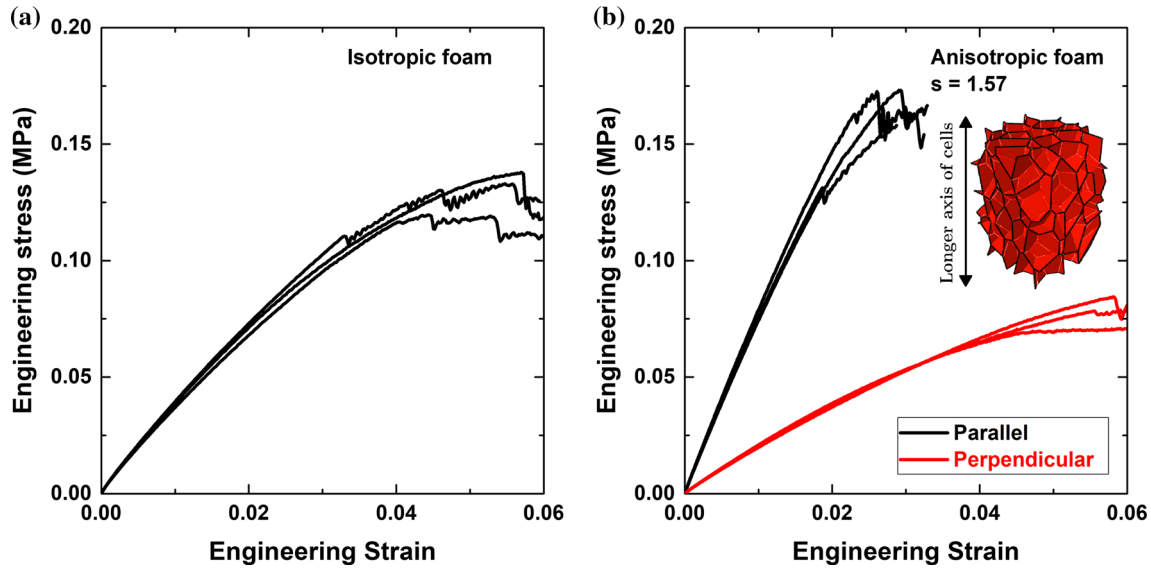
Figure 2 **a** Engineering stress versus engineering strain curves in compression of an isotropic foam. **b** *Idem* of an anisotropic foam with a cell aspect ratio of $s = 1.57$ in the directions parallel and perpendicular to the longer axis of the cells. Data for three different cell realizations are presented in each case.

anisotropic foam was much stiffer when deformed parallel to the longest axis of the cells, and a sudden drop in the stress was observed after the peak stress. The mechanical response in the perpendicular orientation was more compliant, the nonlinearity in the stress–strain curve started earlier, and the plateau stress was also significantly reduced. Moreover, no sudden drop in the stress was detected after the plateau stress was attained.

The influence of a number of microstructural parameters (distribution of solid material between struts and walls, foam density, cell size distribution, strut shape as well as cell aspect ratio) on the elastic modulus, E, and the plateau stress, σ_{pl}, was ascertained by means of the numerical simulations. The elastic modulus, E_s, and the yield strength, σ_{ys}, of the solid material in all simulations were 2.4 GPa and 110 MPa, respectively. Nevertheless, the results of the parametric study are expected to be applicable when $\sigma_{ys}/E_s < 0.05$, which include most polymers and metals. The baseline parameters that define the properties of the foam in the parametric study were the following. The average foam relative density, ρ/ρ_s, was 2.52% and the fraction of solid material in the struts, ϕ, was 0.6. The cell size followed a Gaussian distribution characterized by an average cell size of 216 μm and a standard deviation of 67 μm. The strut shape was given by Eq. (5). These parameters were used in all the simulations if not indicated

otherwise. For each specific configuration of parameters, three different statistical realizations of the RVE were simulated to check the variability of the results and the average values were used. The results of the parametric study are presented below.

Fraction of solid material in the struts

The fraction of solid material contained in the struts, ϕ, is known to have a large effect of the mechanical properties of the foam [10, 13], and this was the first parameter analyzed. Simulations were carried out for $0.2 \leq \phi \leq 1$ (where $\phi = 1$ stands for an open-cell foam) and relative foam densities in the range $0.025 \leq \rho/\rho_s \leq 0.2$. The average results of the elastic modulus, E, (normalized by E_s) and of the plateau stress, σ_{pl}, (normalized by σ_{ys}) corresponding to three different realizations are plotted in Fig. 3a, b as a function of ϕ. The plateau stress of the foam will be approximated by the stress at the onset of plastic instability in all cases. The simulations show that both the stiffness and the plateau stress of the foam increase as ϕ decreases and material is moved from the struts to the cell walls for a constant value of the relative density. The cell walls, which are connected to the struts, increase the bending stiffness and the critical load for plastic buckling of the latter and improve the overall mechanical properties of the foam.
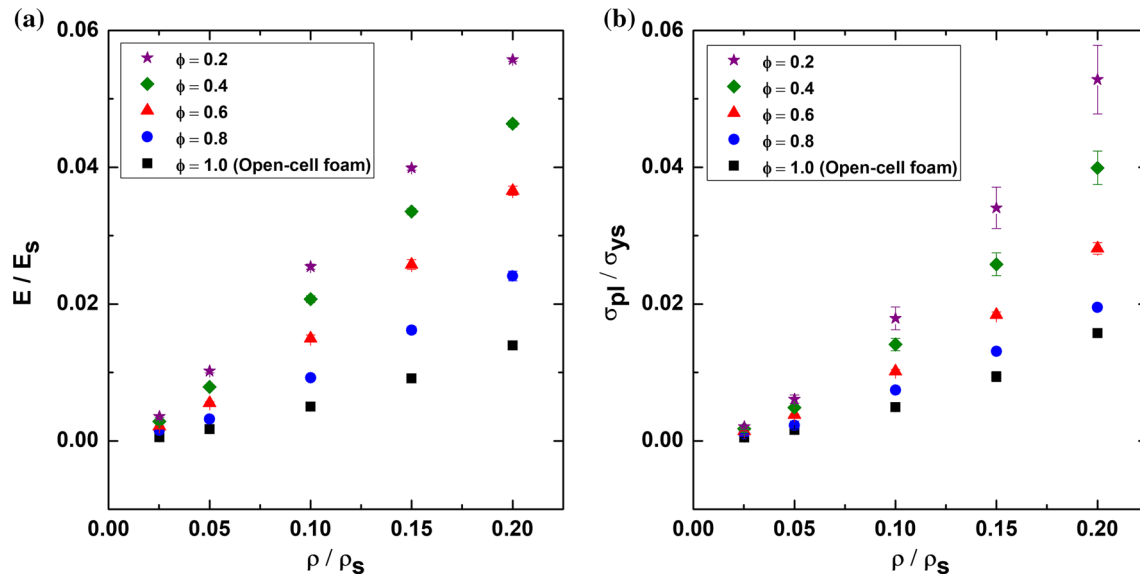
Figure 3 Influence of the fraction of solid material in the struts, ϕ, on the mechanical properties of isotropic foams for different relative foam densities, ρ/ρ_s. **a** Normalized elastic modulus, E/E_s. **b** Normalized plateau stress, σ_{pl}/σ_{ys}. The error bars correspond to the standard deviation of the simulation results for three different realizations.

Cell size distribution

The cell size distribution of the foam was characterized by a Gaussian function with an average cell size of 216 μm and different values of the standard deviation SD (normalized by the average cell size, μ) $0.001 < SD/\mu < 0.5$. The influence of the width of the cell size distribution on both the normalized elastic modulus and the plateau stress is shown in Fig. 4a, b, respectively. In general, the influence is negligible and only an slight increase in both the elastic modulus and the plateau stress was found for uniform cell size distributions (SD = 0.001) which was more noticeable for larger relative foam densities ($\rho/\rho_s \geq 015$). Overall, the influence of this microstructural factor on the mechanical properties is clearly minor.

Strut shape

The shape of the struts in the baseline simulations followed the function $f(x/L)$ in Eq. (5), which was obtained from experimental data provided by X-ray computed microtomography [11]. However, it is important to assess the influence of this factor on the foam mechanical response, as it may change significantly from one type of foam to other (e.g., polymeric vs. metallic) or depending on the manufacturing process. Thus, three different strut shapes (depicted

in Fig. 5) were used to determine the normalized elastic modulus and plateau stress of isotropic foams with different densities ($0.025 \leq \rho/\rho_s \leq 0.2$). Together with the experimental average strut shape (denominated shape 2 in the figure), two other shapes were used for the simulations (Fig. 5). They corresponded to the extremes of the experimental results obtained by X-ray microtomography [11]. The effect of the strut shape on the mechanical response was analyzed in closed-cell foams ($\phi = 0.6$) and open-cell foams ($\phi = 1$).

The elastic modulus and the plateau stress of the foams with different strut shapes are plotted in Fig. 6a, b, respectively, for open-cell foams and Fig. 6c, d for closed-cell foams. The influence of the strut shape was negligible in the range of $0.025 \leq \rho/\rho_s \leq 0.2$. It was found that the changes of strut shape according to Fig. 5 led to a variation $\leq 7\%$ in A_0. This difference was minimum, and the mechanical response of the foams was not influenced.

Cell anisotropy

Finally, the influence of the cell anisotropy on the mechanical properties of the foam was analyzed by means of computational homogenization. The anisotropy of the foam was characterized by the parameter s which stands for the aspect ratio of the elongated cells defined as the average cell length in the loading
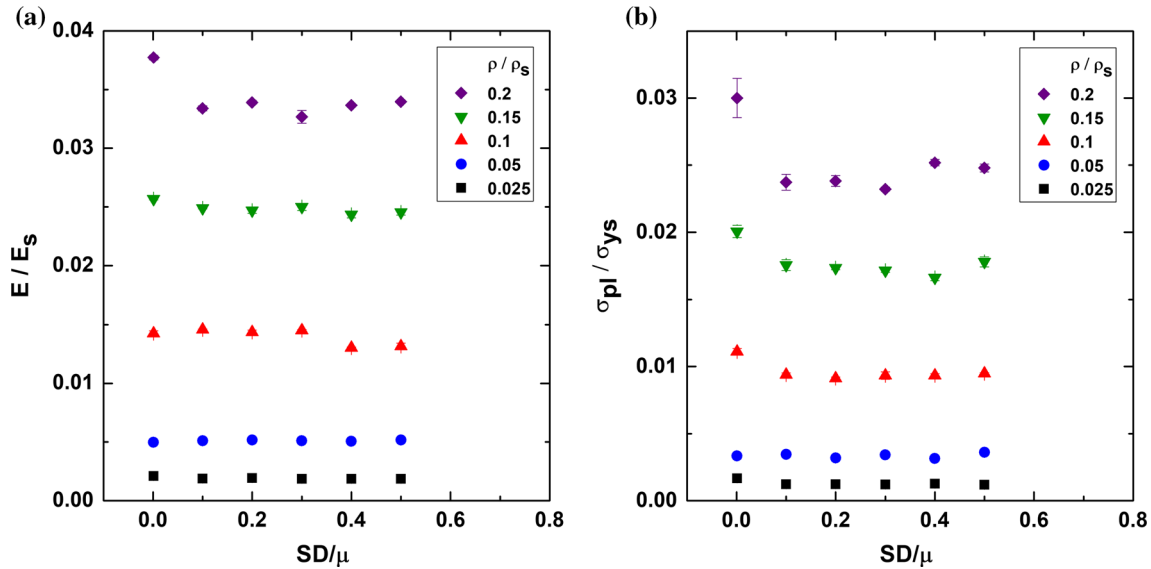
Figure 4 Influence of the width of the cell size distribution (characterized by the standard deviation SD) on the mechanical properties of isotropic foams for different relative densities of the foam, ρ/ρ_s. **a** Normalized elastic modulus, E/E_s. **b** Normalized plateau stress, σ_{pl}/σ_{ys}. The error bars correspond to the standard deviation of the simulation results for three different realizations.
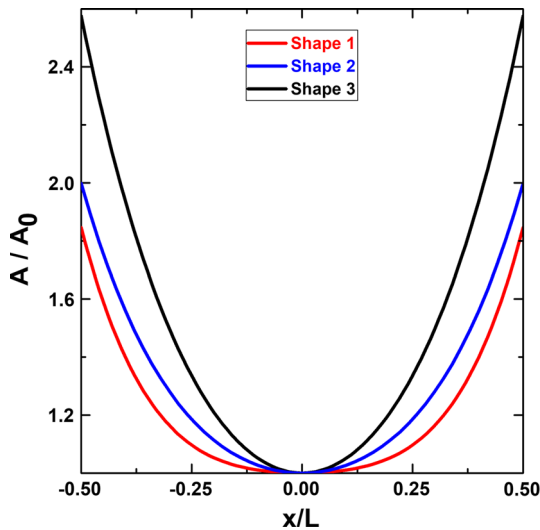
0.2, 0.4, 0.6, 0.8 and 1 and different relative densities ($\rho/\rho_s = 0.025, 0.05, 0.1, 0.15$ and 0.2). Each point in these plots is the average of three different realizations. The rest of the parameters of the foam (cell size distribution, strut shape) correspond to the baseline values indicated above.

The results in both figures indicate the strong influence of the cell aspect ratio on the mechanical properties of the foam, in agreement with the experimental data in the literature [12, 18–20]. In general, both the elastic modulus and the plateau stress increased with s, leading to a strong anisotropy in the mechanical properties of the foam (because both properties simultaneously increase along the direction with $s > 1$ and decrease in the perpendicular orientation with $s < 1$). The only exception to this behavior is found in the plateau stress of open-cell foams (Fig. 8e) for large aspect ratios ($s \geq 1.5$) which seems to be fairly independent of the aspect ratio. This behavior is associated with the reduction in the central section of the struts when they have been subjected to a large elongation. As a result, the increase in the buckling stress due to the orientation of the struts along the loading axis (normal forces dominate over bending forces) is balanced by the reduction in the central cross-sectional area of the struts, which facilitates buckling. This behavior is not found in the case of closed-cell foams because the

Figure 5 Strut shapes used in the simulations. They are defined by $f(x/L)$, Eq. (5), which expresses the variation of the strut cross-sectional area A (normalized by the area of the central section, A_0) as a function of the distance to the center of the strut, x (normalized by the strut length, L).

direction divided by the average cell length in the perpendicular direction [12]. Typical values of the s are in the range $0.5 \leq s \leq 2$ [12], and the parametric study covered this range. The normalized values of the elastic modulus and of the plateau stress of the foams as plotted as a function of s in Figs. 7 and 8, respectively, for different values of $\phi =$

presence of cell walls compensates the reduction in the cross-sectional area of the struts.

Surrogate models

The surrogate models developed by Gibson and Ashby [13] for the elastic modulus the plateau stress of foams, Eqs. (1) and (2), respectively, were based on very simple assumptions and could provide rough estimates but not accurate values (unless the

parameters of the model were adjusted by comparison with experimental data for a given type of foam). The estimates of Köll and Hallström [10], Eq. (3) for the elastic modulus of isotropic foams were much more accurate; insofar they were obtained from
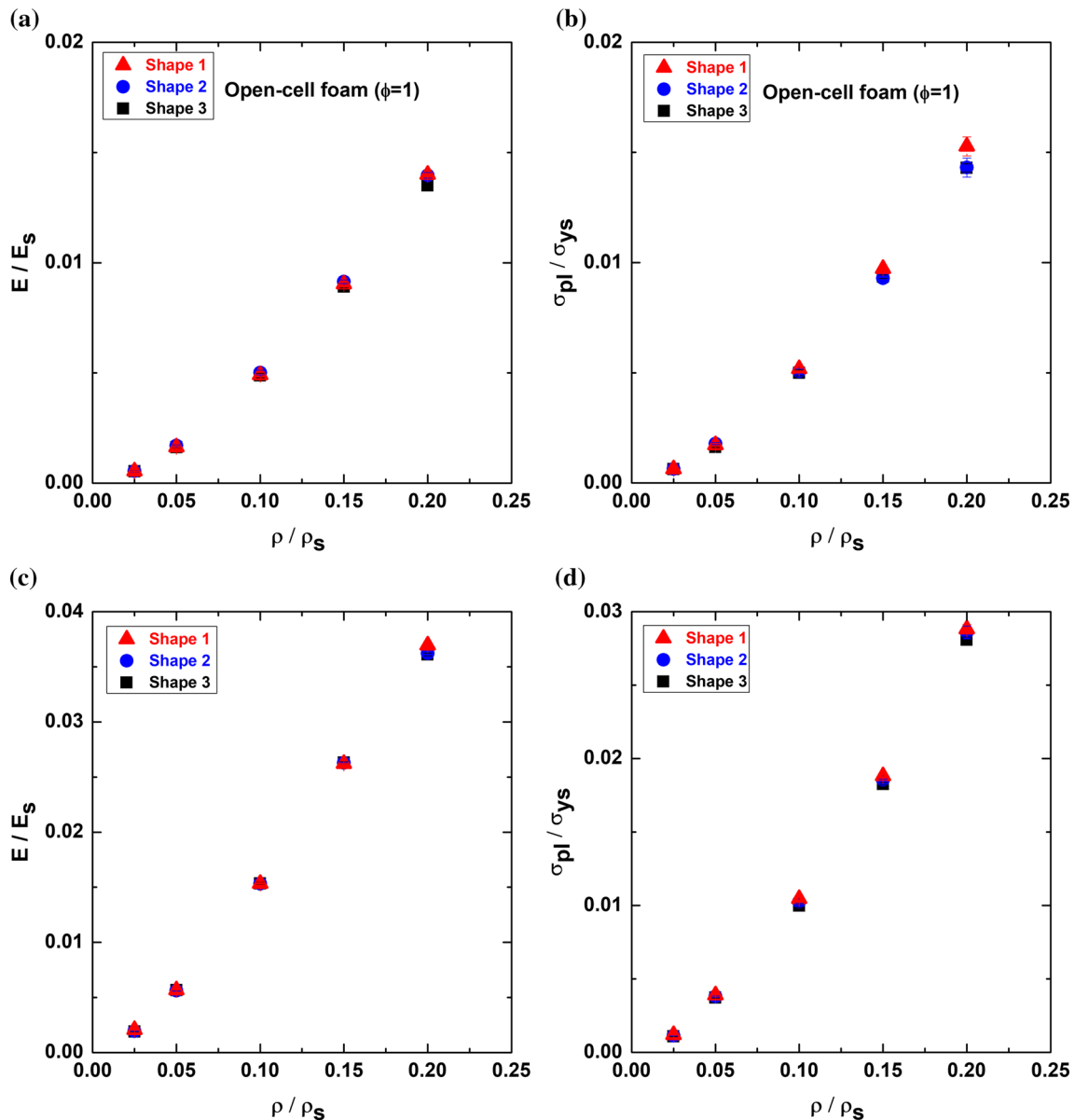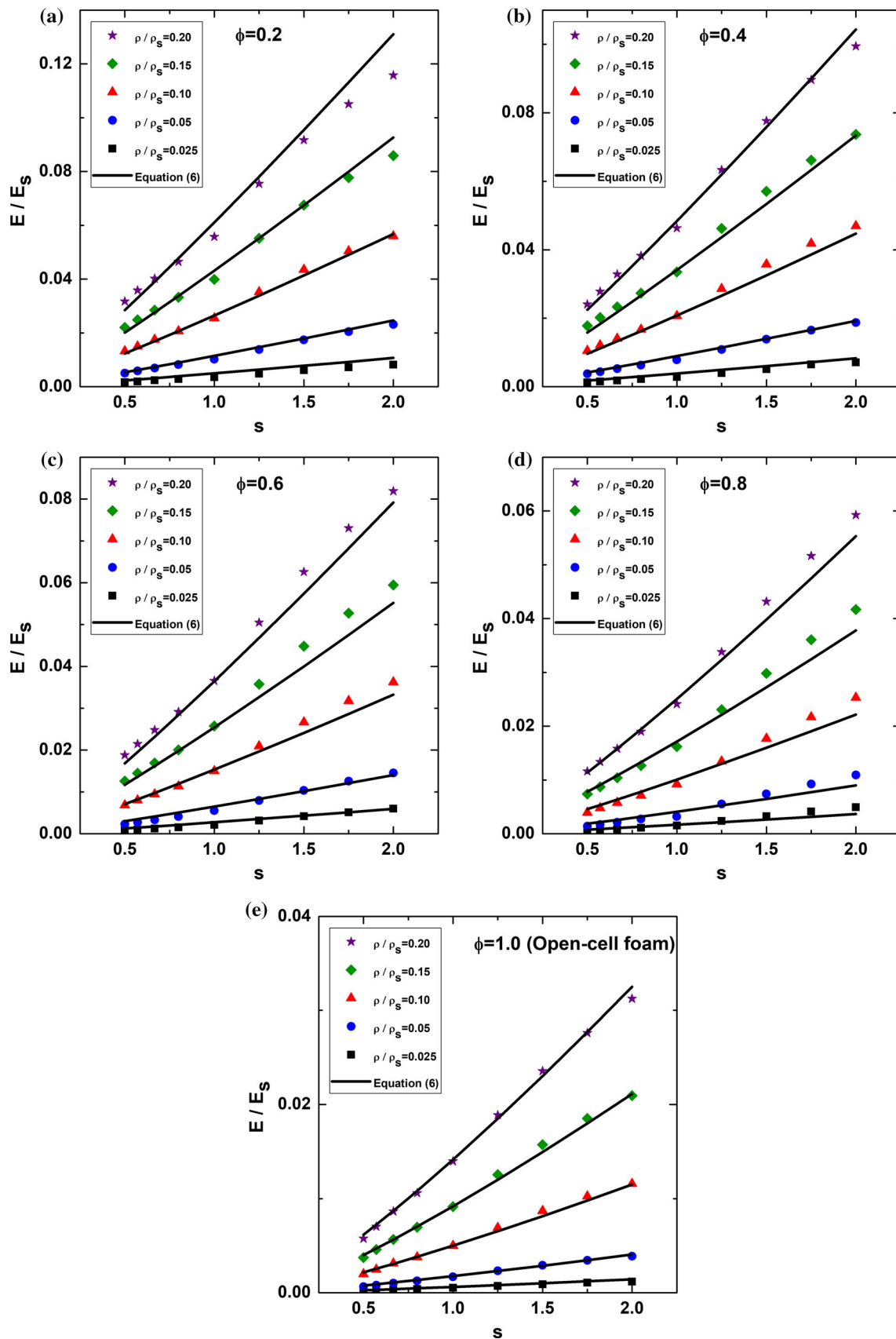

Figure 6 Influence of the strut shape on the mechanical properties of isotropic foams for different foam densities. **a** Normalized elastic modulus, E/E_s, for $\phi = 1$. **b** Normalized plateau stress, σ_{pl}/σ_{ys}, for $\phi = 1$. **c** Normalized elastic modulus, E/E_s, for $\phi = 0.6$. **d** Normalized plateau stress, σ_{pl}/σ_{ys}, for $\phi = 0.6$.
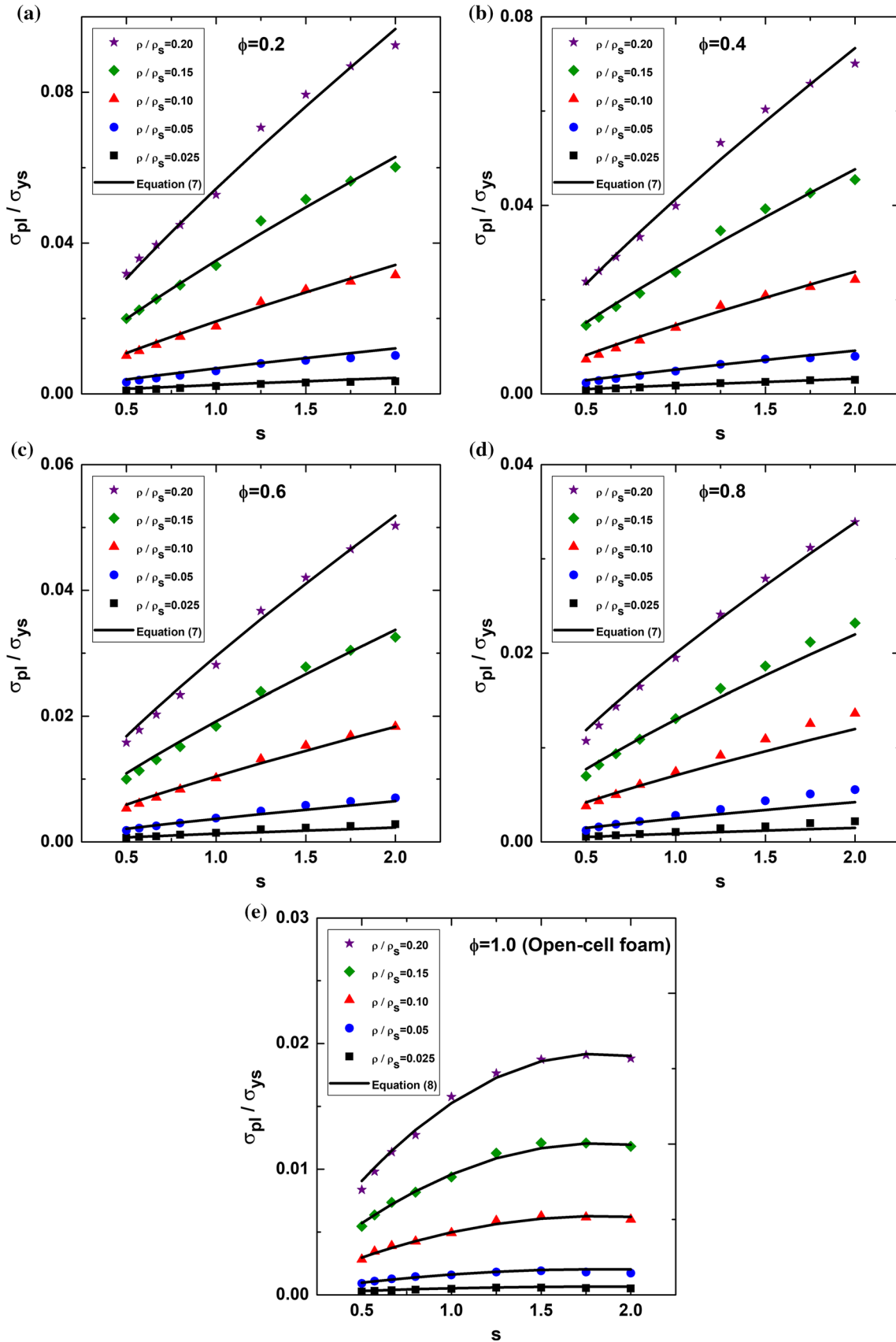
◄**Figure 8** Influence of the cell aspect ratio s on the normalized plateau stress of the foam, σ_{ps}/σ_{ys}. **a** $\phi = 0.2$, **b** $\phi = 0.4$, **c** $\phi = 0.6$, **d** $\phi = 0.8$, **e** $\phi = 1$ (open-cell foam). The solid lines correspond to Eq. (7) for closed-cell foams and to Eq. (8) for open-cell foams.

Table 1 Constants of Eqs. (6), (7) and (8) to determine the elastic modulus and the plateau stress of closed-cell and open-cell foams

C_1	C_1'	C_3	C_4	C_5	C_6	C_7
0.158	0.5155	0.156	0.760	1.614	− 0.077	0.282

numerical simulations of RVEs of the foam microstructure. However, they did not include the effect of the anisotropy and surrogate models for the plateau stress are not available in the literature.

Thus, the results of the numerical simulations plotted in Figs. 7 and 8 for the elastic modulus and the plateau stress, respectively, were used to develop surrogate models for these properties. The models depend on the three main parameters that control the properties of the foam, namely relative density (ρ/ρ_s), fraction of solid material in the struts (ϕ) and aspect ratio (s). In the case of the elastic modulus, the experimental results were reproduced by the function

$$\frac{E}{E_s} = C_1 s^{1.2}\left(\phi\frac{\rho}{\rho_s}\right)^{1.5} + C_1' s^{1.1}(1-\phi)\left(\frac{\rho}{\rho_s}\right)^{1.2} \quad (6)$$

for both open- and closed-cell foams.

The plateau stress for closed-cell foams could be obtained as

$$\frac{\sigma_{pl}}{\sigma_{ys}} = C_3 s^{0.6}\phi^{3.5}\left(\frac{\rho}{\rho_s}\right)^{1.5} + C_4 s^{0.8}(1-\phi)\left(\frac{\rho}{\rho_s}\right)^{1.5} \quad (7)$$

while it was better reproduced in the case of open-cell foams by

$$\frac{\sigma_{pl}}{\sigma_{ys}} = \left(\frac{\rho}{\rho_s}\right)^{C_5}\left(C_6 s^2 + C_7 s\right). \quad (8)$$

The constants in these equations can be found in Table 1. The predictions of Eqs. (6), (7) and (8) are compared with the results of the numerical simulations in Figs. 7 and 8 ,and the agreement is very good for the whole range of densities, cell aspect ratios and anisotropies covered by the simulations.

It is worth noting that the numerical simulations and Eq. (8) predict a maximum value of the plateau stress of open-cell foams (Fig. 8e) for a given value of ρ/ρ_s as a function of the anisotropy aspect ratio s. It is believed by authors that the optimum values of the aspect ratio that maximize the elastic modulus or the plateau stress will be found for all open-cell foam densities if the numerical results plotted in Figs. 7 and 8 are extended to the higher values of s.

Conclusions

A modeling strategy, based on a computational homogenization strategy previously developed [11], has been used to carry out a parametric study of the influence of microstructural factors on the mechanical behavior of open- and closed-cell foams. The approach is based in the numerical simulation of the mechanical behavior in compression of an RVE of the microstructure, which includes the most relevant microstructural details, namely the cell size distribution, cell shape, strut shape as well as the fraction of solid material in the cell walls and in the struts.

The strategy was used to carry out a parametric study of the influence of the density and of the microstructural parameters indicated above on the elastic modulus and the plateau stress of the foam. It was found that these properties depended mainly on the density, fraction of material in the cell walls and struts and the cell shape, and were largely insensitive to the cell size distribution and the strut shape. Building on these numerical results, accurate surrogate models were proposed for the elastic modulus and the plateau stress of open- and closed-cell foams. They relate the microstructural features of the foam to the macroscopic properties and can be used for the design of foams with optimized properties for particular applications.

The computational homogenization strategy which supports the surrogate models was validated against experimental results in polyurethane foams [11], but it can be extended to other polymeric or metallic foams insofar the ratio between the yield strength and the elastic modulus of the solid material leads to an elasto-plastic behavior $\sigma_{ys}/E_s < 0.05$. Future work will try to extend the simulations up to larger strains, including the plateau region and the final densification stage. This will require to include the contact forces between cells and the effect of the air pressure within the cells in the case of flexible, closed-cell foams.

Acknowledgements

References

[1] Berlin A (1980) Chemistry and processing of foamed polymers. Springer, Berlin

[2] Mills N (2007) Polymer foams handbook. Butterworth-Heinemann, Oxford

[3] Daniel I M, Gdoutos E, Rajapakse Y (2009) Major accomplishments in composite materials and sandwich structures. Springer, Berlin

[4] Banhart J (2001) Manufacture, characterisation and application of cellular metals and metal foams. Prog Mater Sci 46:559–632

[5] Banhart J (2008) Porous metals and metallic foams: current status and recent developments. Adv Eng Mater 10:775–787

[6] Tekoglu C, Gibson LJ, Pardoen T, Onck PR (2011) Size effects in foams: experiments and modeling. Prog Mater Sci 56:109–138

[7] Chen Y, Das R, Battley M (2015) Effects of cell size and cell wall thickness variations on the stiffness of closed-cell foams. Int J Solids Struct 52:150–164

[8] Redenbach C, Shklyar I, Andrä H (2012) Laguerre tessellations for elastic stiffness simulations of closed foams with strongly varying cell sizes. Int J Eng Sci 50:70–78

[9] Köll J, Hallström S (2014) Generation of periodic foam models for numerical analysis. J Cell Plast 50:37–54

[10] Köll J, Hallström S (2016) Elastic properties of equilibrium foams. Acta Mater 113:11–18

[11] Marvi-Mashhadi M, Lopes CS, LLorca J (2018) Modelling of the mechanical behavior of the polyurethane foams by means of micromechanical characterization and computational homogenization. Int J Solid Struct 146:154–166. https://doi.org/10.1016/j.ijsolstr.2018.03.026

[12] Marvi-Mashhadi M (2018) Multiscale characterization and modelling of polyurethane foams. PhD thesis, Polytechnic University of Madrid

[13] Gibson L J, Ashby M F (1999) Cellular solids: structure and properties. Cambridge University Press, Cambridge

[14] Lautensack C (2007) Random Laguerre tessellations. PhD thesis, Universitt Karlsruhe

[15] Xue X, Righetti F, Telley H, Liebling TM, Mocellin A (1997) The Laguerre model for grain growth in three dimensions. Philos Mag B 75:567–585

[16] Abaqus (2016) Analysis User's Manual, version 6.13, Dassault Systemes

[17] Jang W-Y, Kraynik AM, Kyriakides S (2008) On the microstructure of open-cell foams and its effect on elastic properties. Int J Solids Struct 45:1845–1875

[18] Amsterdam E, vanHoorn H, DeHosson J, Onck P (2008) The influence of cell shape anisotropy on the tensile behavior of open cell aluminum foam. Adv Eng Mater 10:877–881

[19] Shulmeister V (1998) Modelling of the mechanical properties of low-density foams. Delft University of Technology, Delft

[20] Huber AT, Gibson LJ (1988) Anisotropy of foams. J Mater Sci 23(8):3031–3040. https://doi.org/10.1007/BF00547486